

## DESIGN OF PC BEAM-COLUMN JOINT APPLIED X-BRACED BARS IN THE SEGMENTED STRUCTURAL SYSTEM

Sijun KIM<sup>a</sup>, Seongsoo LEE<sup>b</sup>, Homin CHUN<sup>c</sup>, Kappyo HONG<sup>a</sup>

<sup>a</sup>Department of Architectural Engineering, Yonsei University, Seoul, 120-749, South Korea

<sup>b</sup>Department of Architecture and Building Engineering, Kunsan National University,  
Kunsan, 573-701, South Korea

<sup>c</sup>Department of Architecture, Chodang University, Muan, 534-701, South Korea

Received 05 Oct 2012; accepted 16 Jul 2013

**Abstract.** This study suggests a joint design using an X-brace bar to identify the stability and structural performance of a precast concrete (PC) beam-column joint design, which may cause problems when used in a segmented PC beam system for a long-span structure. For this, an experimental PC beam-column model at half scale was designed and verified for applicability of X-braced bars in a panel zone. While previous studies suggested the development of a long-span structural system using precast concrete (PC) and described the problems with PC beam-column joints, this study proposes a solution to improve the structural stability and performance of a PC beam-column joint design and conducts analytical verification.

**Keywords:** long-span, Gerber beam, X-brace, panel zone, PC beam-column joint, precast concrete, segmented PC beam system.

### Introduction

A precast structural system (PC system) can generally be applied only when the span between columns is less than 15–16 meters because of the limitations of transportation and the capacity of lifting equipment (AHS 2007). For example, to create a PC structural system with a span greater than 17 meters, the total length of the vehicle which transports the PC members from the plant to the construction site should measure less than 17 meters from the vehicle's front bumper to the rear end of the PC members on board, according to the Road Traffic Act (Korea, Japan, USA, Canada, Germany, England, France: width 2.5~2.6 m, height 2.5~3.0 m, length 14~16 m, weight 20~30 ton). For these reasons, long-span structural systems with steel and composite structures are under consideration in the architectural field. Steel and composite structures have some advantages in terms of workability and convenience. However, they also have disadvantages in terms of vibration isolation and economic benefits, which are lower than those of PC structure systems (Murray 1975; Hal *et al.* 1991). To resolve these problems, a new structural system is required.

A segmented PC beam system is one method of handling spans greater than 17 meters and the associated traffic limitations. The segmented PC beam system was developed as a solution to the problems of transportation

and lifting of PC beams longer than 17 meters. The stability of this system in general structures has been studied (Park *et al.* 2005). The proposed structural system in this research uses a method segmenting a long girder into both-end cantilevered beams and a central simple beam using the classical structural concept of the Gerber beam (Cowan, Smith 2004). In the segmented PC beam system suggested (Lee *et al.* 2010a; Hong *et al.* 2010), the center of the PC beam-column joint, the panel zone, does not contain any concrete to allow cross-connection with columns. Use of this system requires verification of stability and structural performance of the PC beam-column joint when a load is applied. With this beam cross-connection in panel zone, a previous study considered the workability of the proposed PC system. Some structural behavior under eccentric loads may require shear reinforcement in the center of the both-end cantilevered beam because a beam connected to a column is subject to eccentric loads during construction, which causes shear deformation in the panel zone of the beam-column joint (Lee *et al.* 2010b).

In this research, an X-braced panel zone is designed and tested for shear reinforcement of the both-end cantilevered beam to investigate the shear deformation of the X-braced panel zone and the associated overall structur-

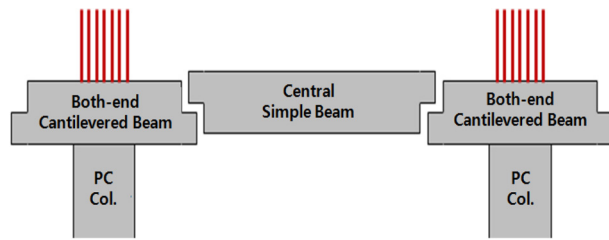


Fig. 1. Concept of the segmented PC beam system

al behavior of the beam-column joint. In addition to the performance evaluation, several methods are discussed to improve the workability and structural performance of the long-span PC system and verify the structural stability and performance of the improved panel zone using a finite element analysis program.

### 1. Segmented PC beam system

#### 1.1. Concept of segmented PC beam

As shown in Figure 1, a segmented PC beam system can secure the moment connection of the beam-column joint by placing the both-end cantilevered beams on the PC columns and then placing a central simple beam on both ends of the cantilevered beams. This system may resolve the transportation problems related to length of PC members and the lifting problems related to weight.

To apply a PC system to structures with a span greater than 17 meters, members should be segmented and assembled on the construction site, which requires sufficient workspace, more time during construction, and additional cost. However, if a continuous beam is designed as a Gerber beam system, instead of using rigid connections, it will not only resolve problems, but also be able to take advantage of the traditional benefits of the Gerber beam. Figure 2 shows a floor frame using a segmented PC beam system. A longer side girder with a span greater than 17 meters is segmented into GG2 (both-end cantilevered beam) and GG1 (central simple beam). The lengths of GG2 and GG1 are about 6–7 and 10 meters, respectively. GG1 is supported on both ends of GG2, and the gaps in the joints are filled with non-shrinking mortar. Since B1, B2, and G1 are no longer than 15 meters, they are not segmented but formed as single members so that they can be built according to the general PC method and design conditions.

The segmented PC beam system provides advantages such as optimized cross-sectional designs of members by segmenting the members at the positions where the positive and negative moments of continuous beams become approximately the same and utilization of the full pretension capacity in PC members which adopt pretension strands (ACI 318-11:2011).

#### 1.2. Design of the beam-column joint

In the both-end cantilevered beam to be assembled over the PC column, the concrete in the central parts of the

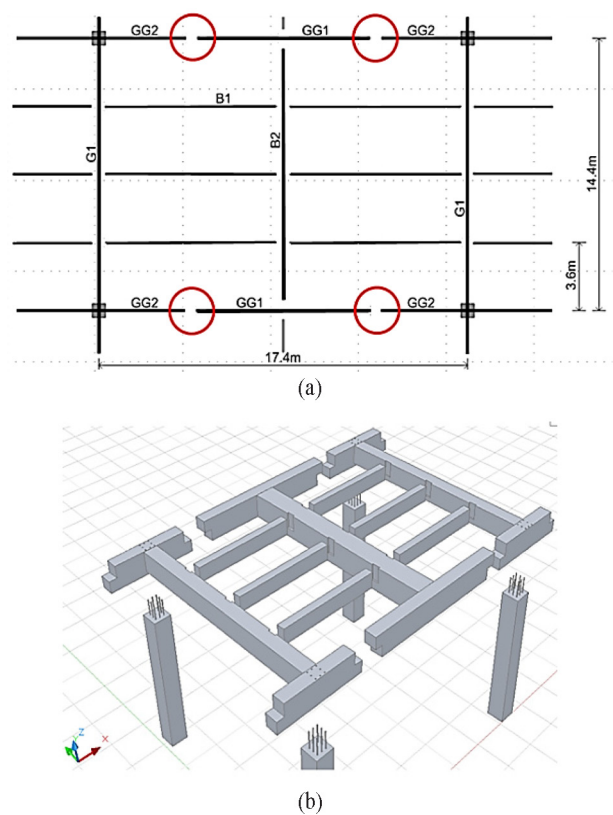


Fig. 2. An example of a segmented PC beam system

beam should be removed, as shown in Figure 3(a), or the through holes should be made for the rebar of the column to pass through, as shown in Figure 3(b). While eliminating the central concrete in the both-end cantilevered beam may make it easier to assemble the beam-column joints, it can also cause deformation of the cantilevered beam during lifting and assembling and requires a wet process whereby the panel zone needs to be filled with concrete on-site. Designing the through holes in the central parts

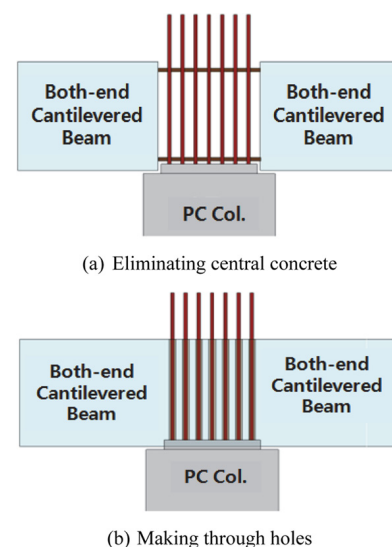


Fig. 3. Types of central parts in both-end cantilevered beams

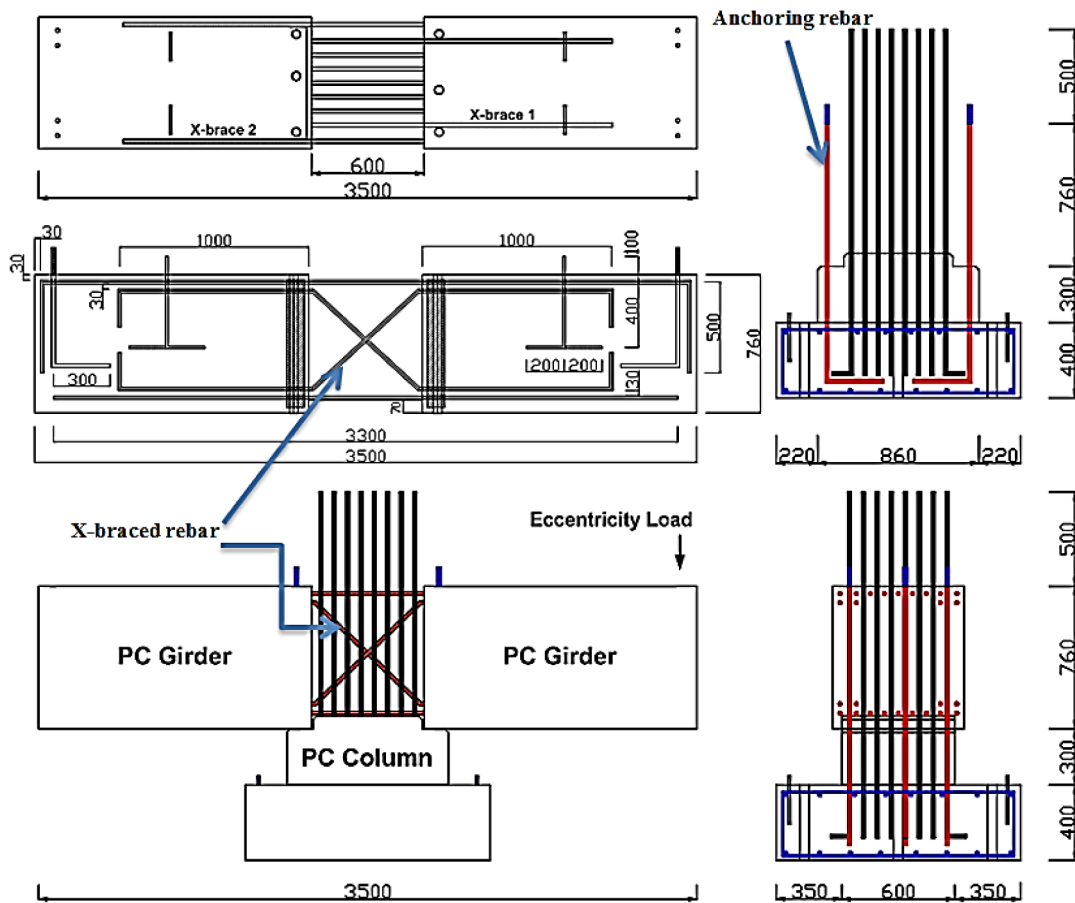


Fig. 4. Dimensions of the specimen

of the both-end cantilevered beam may ensure rigidity in the beam-column joint but requires precision in design and construction because every column rebar should be matched with the exact location of the holes (Nilson *et al.* 2003). Since construction workability is considered essential, the system in Figure 3(a) was selected for this research.

## 2. Experiment

### 2.1. Description of experiment

This study attempts to find design solutions for a micro vibration industrial facility using a long PC system (Kim *et al.* 2009). The micro vibration industrial facility must be designed with large beams with widths greater than 1 meter and heights greater than 1.5 meters to support the axial load of columns supporting the cleanroom and the weight of machinery. The experiment was carried out on a half-scale model due to the limited space of a laboratory and capacity of actuators. Figure 4 shows the dimensions of the specimen reduced by half (KCI 2007). The names of each member are shown in Figure 2.

#### 1. GG2 (1400 × 1520 mm → 700 × 760 mm)

The six (3 + 3) through holes for anchoring rebar were designed to prevent overturning of the both-end cantilever.

#### 2. C1 (1200 × 1200 → 600 × 600)

To form a moment-resistance mechanism with GG2, the 70 mm high compression protruding concrete was designed at the upper part of the PC column.

#### 3. Anchoring rebar

(3-D35,  $F_y = 500 \text{ MPa}$  → 3-D19,  $F_y = 400 \text{ MPa}$ )

Three anchoring pieces of rebar were designed on each of two opposite edges of the PC column to prevent overturning of GG2 under eccentric load.

#### 4. Strength of material

Nominal compression strength of concrete = 35 MPa, yield strength of rebar = 400 MPa.

Figures 5, 6, and Table 1 show the sensor locations. Eighteen strain gauges were attached to the rebar and concrete. Four displacement transducers were installed

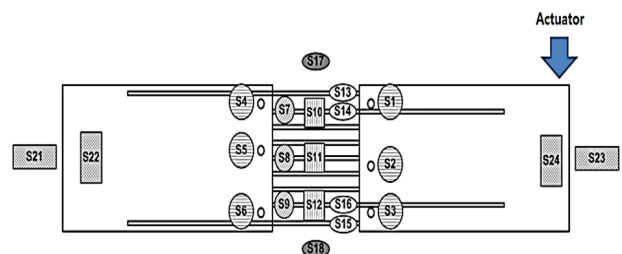


Fig. 5. Sensors arrangement

Table 1. Sensor locations

Sensor type	Sensor No.	Location
Strain gauges	S1-S6	Anchoring rebars
	S7-S9	Tension rebars (upper) in GG2
	S10-S12	Compression rebars (lower) in GG2
	S13-S16	X-braced rebars
	S17-S18	Protruded concrete in C1
Displacement transducers	S21, S23	Horizontal displacement on both sides of beam
	S22, S24	Vertical displacement on both sides of beam



Fig. 6. Strain gauges

on the sides and bottoms of both ends of GG2 to check for excessive torsion of the specimen.

The phases of eccentric loads, which are applied to the both-end cantilevered beam during construction of the segmented PC beam system, can be classified as shown in Figure 7.

As shown in Table 2, loads applied to the specimen are calculated considering the scale-down from the expected construction loads in each step of a building as follows (Harris, Sabnis 1999):

$$P^{exp} = P^{act} \frac{\varphi M_n^{exp}}{\varphi M_n^{act}} \left( \frac{2L}{L} \right) = P^{act} \frac{635.4}{5790} \times 2 \cong 0.2 \times P^{act}, \tag{1}$$

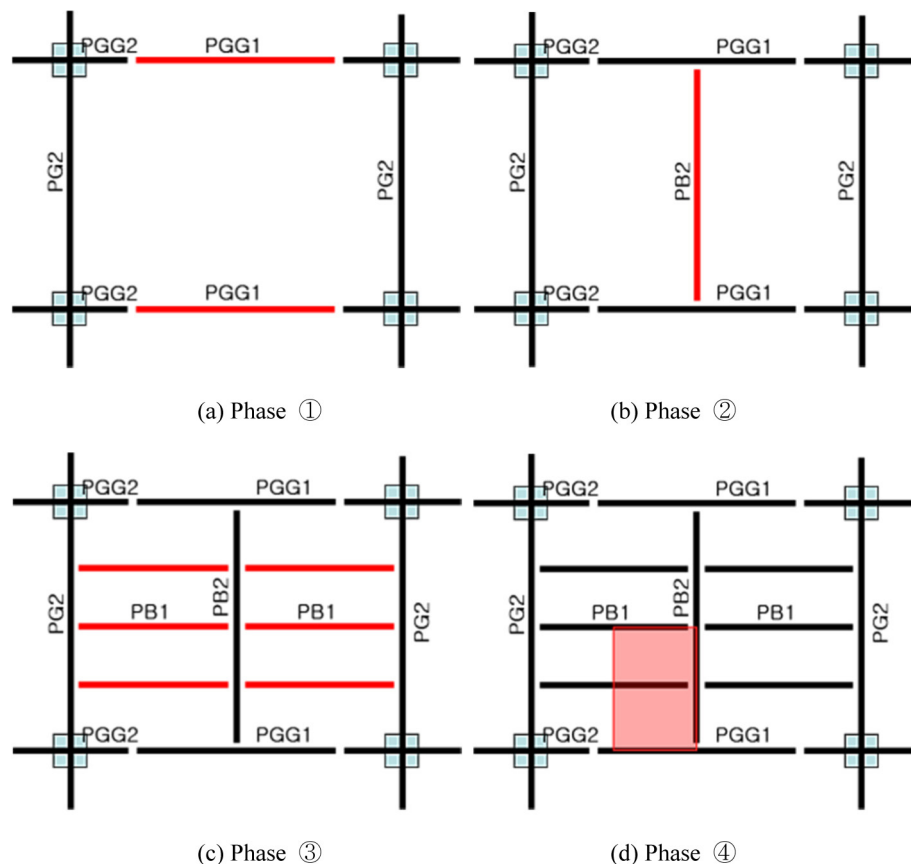


Fig. 7. Phases in the construction of a segmented PC beam system

Table 2. Actual and experimental loads

Construction phase	Actual construction load (kN)	Applied experimental load (kN)
Placing PGG1 on only one span	285	57
Placing PB2 on one side after finishing PGG1 placement	152	30
Placing PB1 on one side after finishing PGG1 and PB2 placement	54	11
Concrete casting on slab	193	38

where  $P^{exp}$  is the maximum experimental load,  $P^{act}$  is the actual construction load,  $\phi M_n^{exp}$  is the moment strength of the reduced PC beam (635.4 kNm; 700 × 760,  $f_{ck} = 35$  MPa,  $F_y = 400$  MPa, 9-D19), and  $\phi M_n^{act}$  is the moment strength of the actual PC beam at half scale (5790 kNm; 1400 × 1520,  $f_{ck} = 35$  MPa,  $F_y = 500$  MPa, 9-D35).

As shown in Figure 8, the eccentric load is applied to one end of the both-end cantilevered beam at the rate of 200 N/sec until the deformation of panel zone applied X-braced rebar happen (Harris, Sarikanth 1980).

## 2.2. Experimental results

### 1. Deformation due to eccentric loading

Deformation due to the eccentric load can be classified into overturning, shear deformation, and cantilever behavior, as shown in Figure 9.

Overturning deformation refers to deformation caused by rigid body motion of both-end cantilevered beams, which rotate on a hinge. Since the opposite side



Fig. 8. View of experimental setup

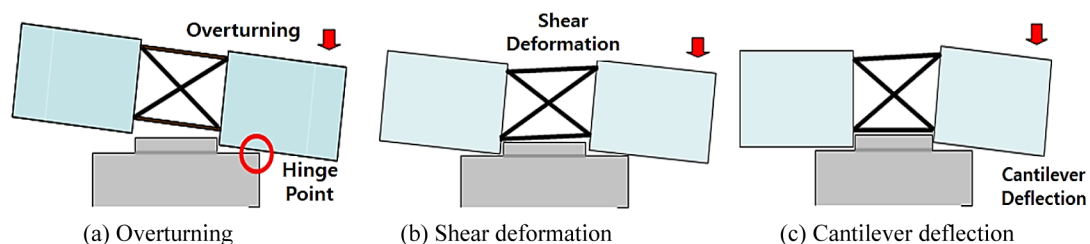


Fig. 9. Types of deformation of GG2 while eccentric loading

of the hinge is longer than the loaded side, upward displacement is greater than the downward displacement (Fig. 9a). Shear deformation is caused in the central part of the panel zone (Fig. 9b). When rigid bodies at both ends rotate at the same angle and there is no vertical displacement in the anchoring rebar, the absolute amount of vertical displacement is equal on both ends. However, since there is a differential local deformation in beam rebar due to shear deformation in the panel zone, and there is actually slight vertical displacement in the anchoring rebar, the absolute amount of vertical displacement on both ends cannot be equal in practice. The cantilever deflection refers to vertical deflection in the cantilever under an eccentric load, as shown in Figure 9c.

Figure 10 shows the results of horizontal and vertical displacement when 73 kN was applied. The vertical downward displacement (S24) of 9.6 mm and upward displacement (S22) of 9.88 mm occurred at both ends of PGG2. The amount of displacement at the eccentric loaded side was slightly larger than that at the opposite side up to about 60 kN, but after the load exceeded 60 kN, the vertical displacement at the opposite side was more greatly increased. As the load (about 73 kN) exceeded 60 kN, buckling on the X-braced rebar was observed, and significant shear deformation began in the panel zone. It can be assumed that the vertical displacement on the opposite side became larger due to the buckling of the X-braced rebar with shear deformation in the panel zone.

### 2. Behavior of anchoring rebar

The anchoring rebar was designed to restrain the overturning caused by the eccentric load on the PC beam in the beam-column joint. The anchoring 3-D19 rebar was embedded in each opposite edge of the PC column. Strain gauges were attached on all pieces of rebar, but one gauge was damaged while the specimen was being

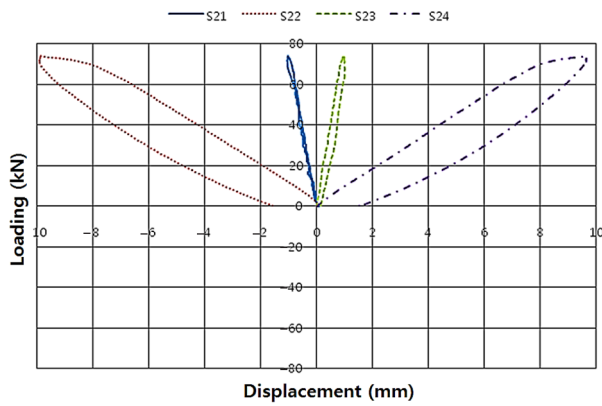


Fig. 10. Displacement curves for eccentric loading

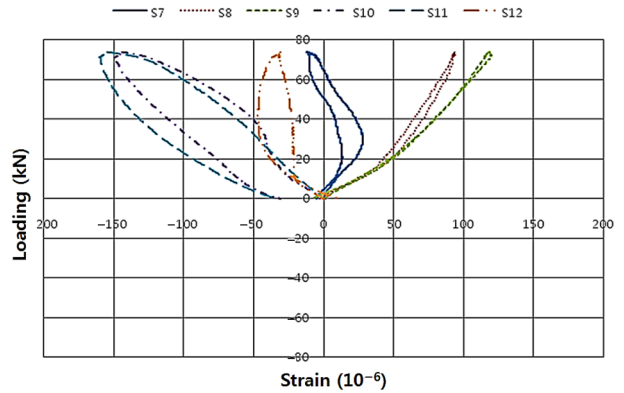


Fig. 12. Strain curves of rebar in PC beams under eccentric load of 73 kN

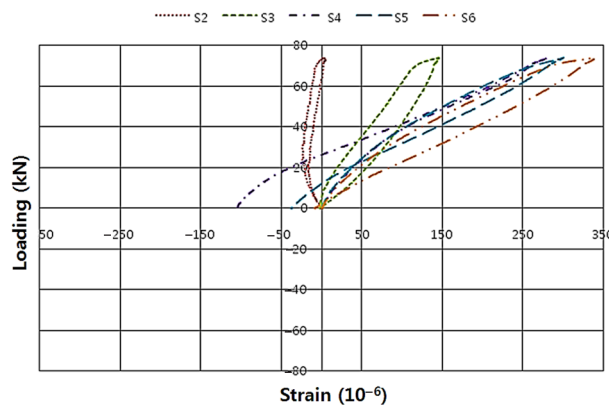


Fig. 11. Strain curves of anchoring rebar under eccentric load

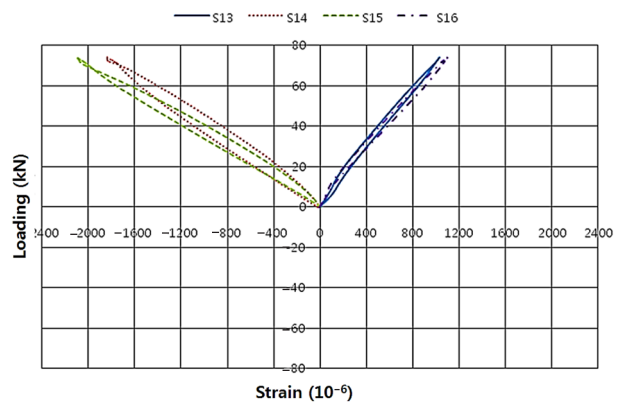


Fig. 13. Strain curves of X-braced rebar of PC beam under an eccentric load of 73 kN

assembled in the laboratory. Therefore, only five signals were acquired, and Figure 11 shows the strain results of S2 to S6.

The average tensile strain of the anchoring pieces of rebar from S4 to S6, that had to resist torsional deformation on the opposite side of the eccentric load, was  $307 \times 10^{-6}$ . The average strain of  $307 \times 10^{-6}$  at a load of 73 kN can be converted into stress, representing approximately 10% of the calculated yield stress. This fact indicates that the stress on the rebar is sufficiently low in the elastic range.

### 3. Performance of main rebar

Figure 12 shows the load-strain relationship of the rebar in the PC beam up to an eccentric load of 73 kN. S7 to S9 are strains measured from the gauges attached to the upper rebar subject to tensile force. S10 to S12 are strains measured from the gauges attached to the lower rebar subject to compressive force. The cantilever motion due to the eccentric load caused tensile force in the upper rebar and compressive force in the lower rebar. Strains below  $155 \times 10^{-6}$  under 73 kN represent a very low state of elasticity.

### 4. Behavior of X-braced rebar

Figure 13 shows the load-strain curves of the X-braced rebar while the specimen was under eccentric load

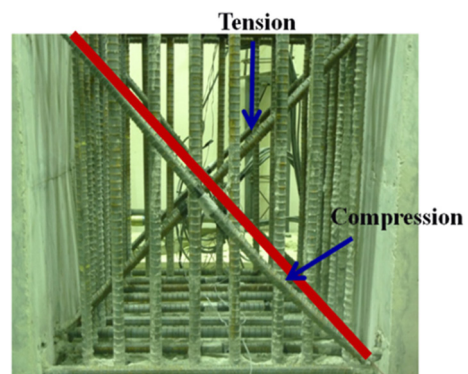


Fig. 14. Buckling in X-braced rebar of PC beam

of 73 kN. Figure 14 shows a situation where shear deformation was occurring after buckling in the X-braced rebar in the panel zone. Strains of approximately  $1100 \times 10^{-6}$  occurred in the X-braced rebar (S16) under tensile stress and those of approximately  $2100 \times 10^{-6}$  (S15) under compressive stress. When the eccentric load was 60 kN, buckling began to be observed in the compression pieces of rebar among the X-braced pieces of rebar. The buckling increased under the continuing force, and at 73 kN, the loading was stopped.

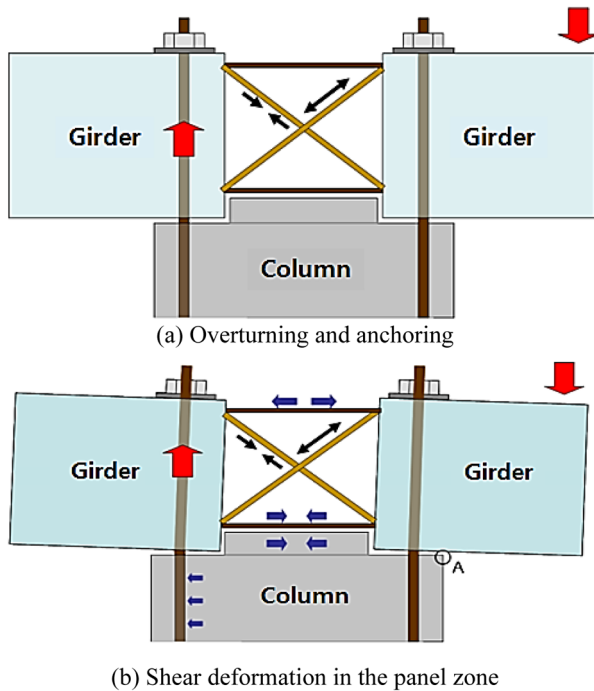


Fig. 15. Stress mechanisms due to overturning and shear deformation

### 5. Cracks in concrete column

There was almost no cracking in the specimen. The contribution of X-bracing is explained in Figure 15. The PC beam was about to overturn clockwise due to the right eccentric load, but overturning deformation was restrained by the anchoring rebar on the opposite side. With the X-braced rebar in the central part of the PC beam, the shape of the entire rigid body of the PC beam could be maintained within the capacity of the X-braced rebar. Therefore, the tensile stress, corresponding to the overturning moment caused by the eccentric load, occurred in the anchoring rebar, and almost no force was generated to remove the cover concrete of anchoring rebar during the rigid-body motion of the PC beam due to the X-braced rebar. However, when the load reached the limit where the X-braced rebar was subject to buckling or yield, shear deformation began to occur in the central part (panel zone) of the PC beam. Then, the overturning deformation for both concrete parts of the PC beam was initiated respectively. Hence, the lateral force which removes the cover concrete was generated.

When the specimen was under an eccentric load of 73 kN, there was no crack in the compressive protruding part of the column. Figure 16 shows the change in the compressive strain of the concrete. Since the overturning deformation of the PC beam was restrained by the anchoring rebar, and the eccentric load acts on the right side, the cantilever motion of the beam occurred and caused tensile stress at the upper rebar and compressive stress at the lower rebar of the beam. This also resulted in compressive stress with strain of about  $30 \times 10^{-6}$  in the compressive protruding part of the PC column.

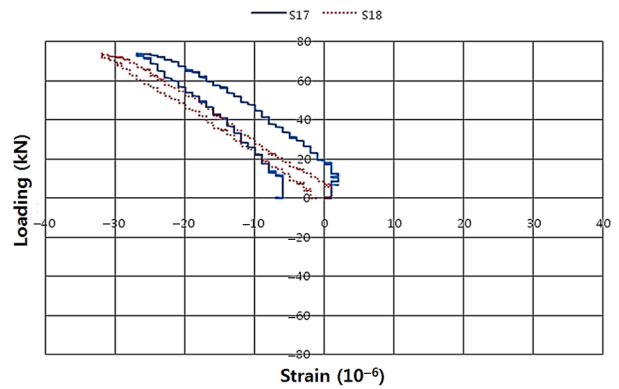


Fig. 16. Strain curves of concrete in the protruding part under an eccentric load of 73 kN

The compressive strain of  $30 \times 10^{-6}$  is very low compared with the limit strain of 0.002 in concrete (Nilson et al. 2003). The compressive stress of the lower part of panel zone, in association with the tensile stress of the upper part caused by the moment due to the eccentric load, was shared with the bottom rebar of the PC beam and protruding concrete, resulting in a very low stress in the protruding concrete.

### 2.3. Improvements in member design

Based on the information and results obtained from the experiment, several improvements are suggested to enhance the workability and structural performance of a PC system with a span greater than 17 m.

#### 2.3.1. Design of X-braced rebar

1. When designing a both-end cantilevered beam for a segmented PC beam system, X-braced rebar should be designed to prevent shear deformation of the panel zone and to secure the rigidity of the both-end cantilevered beam.

2. Since the panel zone of GG2 intersects with the pieces of rebar of the PC column, too many pieces of rebar or too narrow spacing may cause interference between the pieces of rebar of the column and those of the beam, which may cause difficulties in assembly. To resolve such difficulties, high-strength and large-diameter rebar can be used for the beam and for the X-braced rebar in order to reduce the number of pieces of rebar required and to widen the rebar spacing.

3. X-braced rebar should be placed symmetrically, and the rebar should be placed in alternating directions. All X-braced rebar need to be arranged right below or above of the beam rebar to avoid interference with column rebar (Fig. 17).

Embedment of X-braced rebar: Since stress is locally concentrated on the bent parts of X-braced rebar under an eccentric load, it is advisable to embed them in concrete at GG2 to share stress with the concrete and to restrain deformation (Fig. 18).

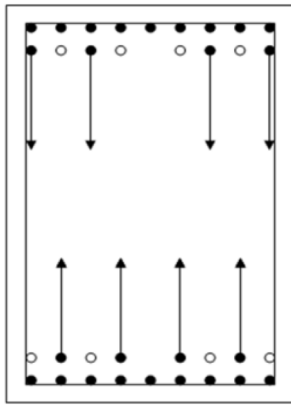


Fig. 17. Symmetric and alternate arrangement of X-braced rebar

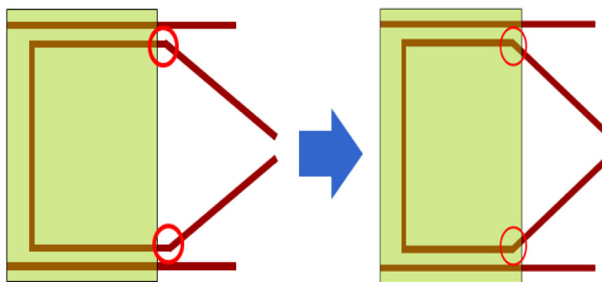


Fig. 18. Bent parts embedded in concrete

### 2.3.2. Design of anchoring rebar

1. It is advisable to use high-strength and large-diameter rebar as anchoring rebar in order to simplify the insertion and installation processes.

2. The rebar should be arranged symmetrically and evenly so that stress is not concentrated on certain pieces of rebar.

3. Point-symmetrical arrangement of anchoring rebar: If anchoring rebar cannot be designed completely symmetrically (left and right, up and down), then they must be placed point-symmetrical so that assembly with GG2 can be conducted regardless of the left-right change of GG2. If anchoring rebar is placed line-symmetrically, GG2 must be lifted and assembled according to the left-right positions of the anchoring rebar (Fig. 19).

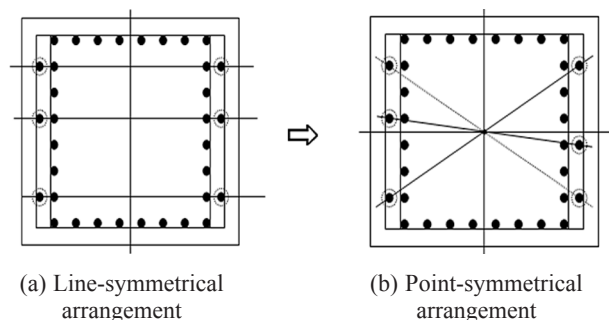


Fig. 19. Arrangements of anchoring rebar

## 3. Improved design model and results of FEM analysis

### 3.1. Verification of analysis modeling

To verify the adequacy of the analysis modeling, the load-strain curves of experimental and analysis model were compared.

#### 1. Modeling

The material properties applied to FEM analysis model were equal to experimental model. The elements used in analysis modeling were 3-D solid elements, Solid187 (10Node Tetrahedral Structural Solid) and Solid186 (20 Node Structural Solid), supported by ANSYS Workbench (ver.11.0). Steel bars embedded in concrete were modeled to behave as a monolithic structure with the members, and the contact surface of the top of the column and the PC beam was applied to the contact condition which is the frictional option. The boundary condition of the model was fixed for the bottom of the column in experiments (Fig. 20).

#### 2. Comparing of Load-Strain Relation

As shown in Figure 21, the load-strain curves of experimental and analysis model were consistent in less than 60kN. In over 60kN, the maximum error of the load-

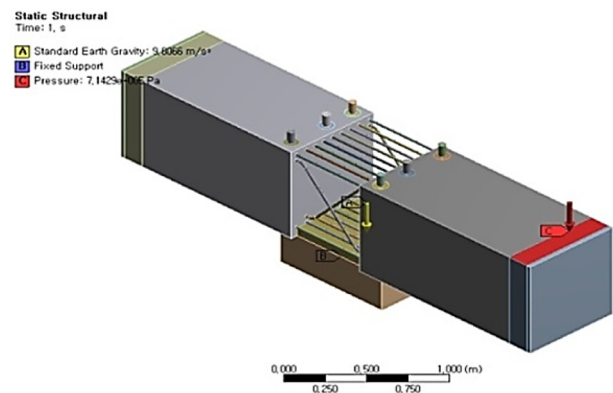


Fig. 20. Load and Boundary Conditions

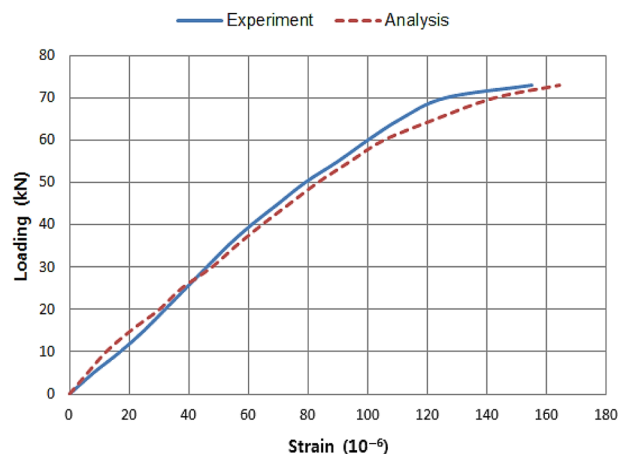


Fig. 21. Load-strain curves of S11

strain curves was approximately 15% because of shear deformation of the panel zone. When considering characteristics of the experiment, the validity of the analysis modeling was confirmed from the comparison of results.

**3.2. Improved design model**

1. While the entire length of the column was not applied to the experimental PC beam-column joint model, this model was designed to verify the structural performance and the applicability of the improved design modeled on a full-length column.

2. To resolve excessive stress concentration in the X-braced model, as shown in Figure 22, the curved parts were inserted into the PC girders to improve the stress concentration in the curved parts.

3. To improve the yield of X-braced bars at the curved parts, as shown in Figure 23, four more bars were placed in addition to the existing four bars to enhance the stability and structural performance of the joint under eccentric load. This modification helped reduce the number of PC girder main bars (from 18 to 12), which are subject to relatively less stress under eccentric load and to maintain the 6 pieces of anchor bars to prevent overturning strain.

4. Figure 24 shows the overall modeling and mesh shape. The modeling method is same as the 4.1.

**5. Boundary Condition and Properties**

The fixed boundary condition was applied to the bottom of the column. Table 3 shows the properties applied to the modeling: for a compressive strength of con-

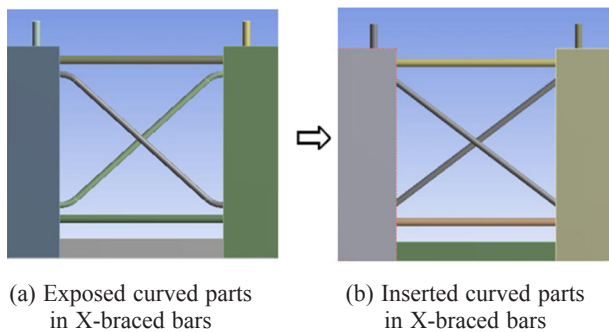


Fig. 22. Modification to the curved parts of X-braced bars

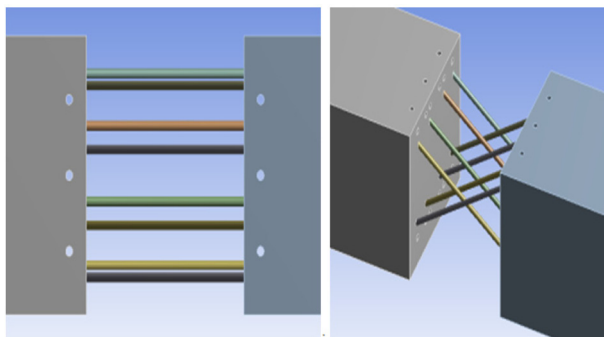


Fig. 23. Increasing X-braced bars (4→8)

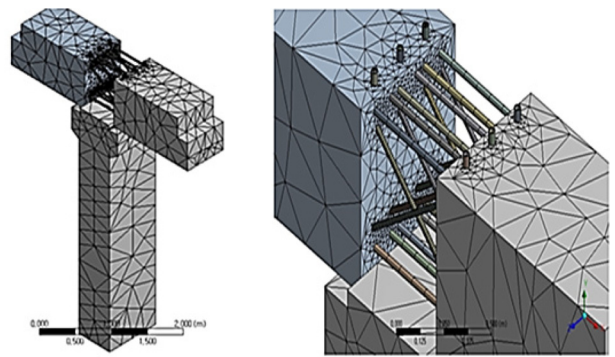


Fig. 24. Overall modeling and mesh shape

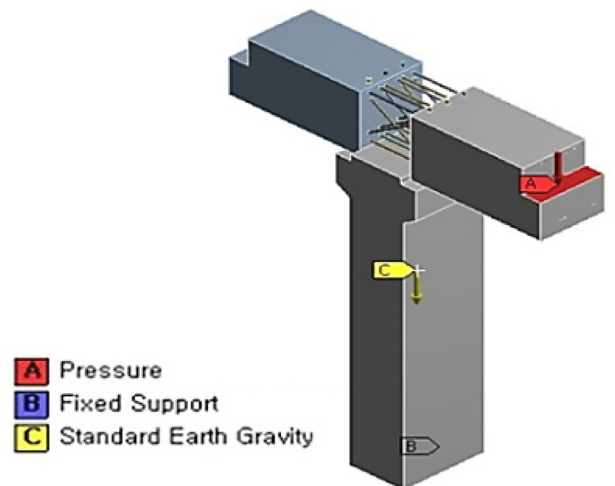


Fig. 25. Applied eccentric load

Table 3. Material Properties

	Concrete [35MPa]	Bars [SHD35]
Modulus of Elasticity	2.6063×1010 N/m <sup>2</sup>	2.0×1011 N/m <sup>2</sup>
Poisson's Ratio	0.167	0.3
Density (ρ)	2,400 kg/m <sup>3</sup>	7,850 kg/m <sup>3</sup>

crete, 35 MPa was applied, and for the bars, SHD35 with strength of 500 MPa was applied, which was greater than the 400 MPa in yield strength applied to the experimental model, considering stability under load.

**6. Applied Load**

As shown in Figure 25, eccentric loads were applied to the experimental load (73 kN) and the maximum load (136 kN) in order to compare with experimental data.

**3.3. Program analysis results of the improved design model**

**1. Stress**

Unlike the experimental model where excessive stress concentration in the curved parts of X-braced bars caused the maximum stress to occur in the curved parts, in the improved design model, as shown Figure 26, the

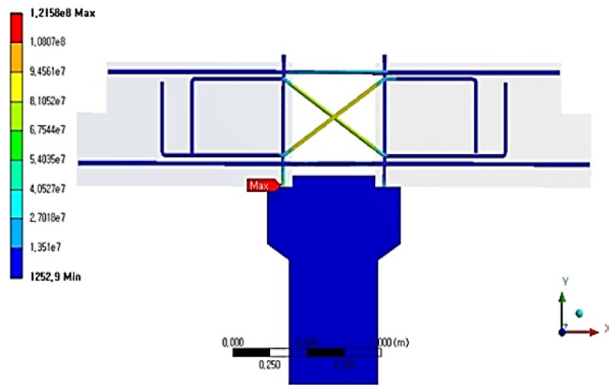


Fig. 26. Location of maximum stress at an eccentric load of 136 kN

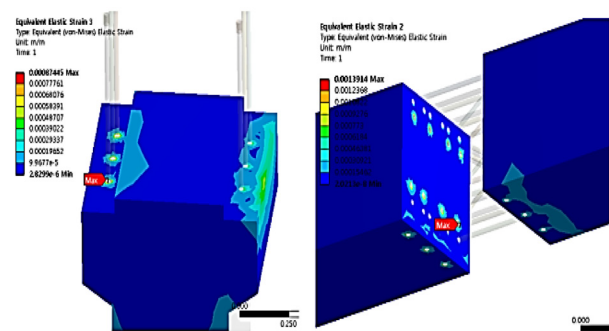


Fig. 27. Strain in PC beam-column interface at an eccentric load of 136 kN

maximum stress occurred in the anchor bars between the PC girder and the column parts when the maximum eccentric load of 136 kN was applied. This study found two reasons for this: First, when the X-braced curved parts were inserted inside the PC girders, the stress concentrated on the curved parts was dispersed. Secondly, additional X-braced bars distributed the stress affecting all X-braced bars, reducing the amount of stress.

By inserting the curved parts of X-braced bars and placing more bars, the improved design, as Table 4 shows, was appropriate for the yield strength (500 MPa) of the bars under any working load.

### 2. Strain

Table 5 and Figure 27 show strains at the PC beam-column interface to identify cracks and flakes of concrete in the same areas under working loads. Under all working loads, the strains were less than 0.003.

### 3. Displacement

As shown in Table 6, the maximum vertical and horizontal displacements at 136 kN were 4.52 mm and

Table 4. Stresses in Load Phases

Load	73 kN	136 kN
Maximum Stress in Anchor Bars (MPa)	61.2	121.6
Maximum Stress in X-braced Bars (MPa)	64.6	120.9

Table 5. Strains in PC Girder-Column Interface

Load	73 kN	136 kN
Strain in PC Girder Surface (m/m)	$2.06 \times 10^{-8} \sim 0.0007$	$2.02 \times 10^{-8} \sim 0.0014$
Strain in Column Overhang (m/m)	$1.53 \times 10^{-6} \sim 0.0004$	$2.83 \times 10^{-6} \sim 0.0009$

Table 6. Displacement by Load Phase

Load	73 kN	136 kN
Vertical Displacement (mm)	2.42	4.52
Horizontal Displacement (mm)	2.91	5.45

5.45 mm, respectively. The results of the analysis at less than 73 kN revealed that the maximum vertical displacement was 2.42 mm, and the maximum horizontal displacement was 2.91 mm. These results represented a decrease both in vertical and horizontal displacement from 6.3 mm (vertical) and 3.7 mm (horizontal), respectively, during the analysis of the experimental model at 73 kN. In addition, as the analysis of the improved model considered the column, the displacement of the column shows that stability and structural performance against deflection were greatly improved compared with the analysis of the experimental model.

## Conclusions

In this paper, an experimental and analytical study was carried out to find methods for applying the long PC system to a building. The conclusions are as follows:

1. Deformation occurring in the both-end cantilevered beam under eccentric load is a combination of shear deformations. The total amount of deformation was 9.6 mm.
2. The strains in the anchoring rebar, beam rebar and concrete were measured as very low states of elastic stress.
3. The X-braced pieces of rebar buckled around 60 kN. The X-braced rebar should be designed with enough safety margin to inhibit shear deformation in the panel zone and to secure the rigidity of the both-end cantilevered beam.
4. Based on the analysis of the experiment results and observations during the experiment, several improvements for member design are suggested to enhance the workability and structural performance of the long PC system.
5. The finite-element analysis of the improved half-scale PC beam-column model showed the results of stress to be lower than the yield strength (500 MPa) under all working loads, with no stress concentration in the curved parts of the X-braced bars. Therefore, it can be concluded that the addition of X-braced bars and the insertion of the curved parts greatly improved structural performance.

6. Although deflection in the column was factored into the overall vertical/horizontal displacements in the finite-element analysis of the improved PC beam-column model, the improved model showed smaller displacements than those in the experimental model.

7. In the finite-element analysis of the improved PC beam-column model, the strain in the PC girder-column interface at all working loads was less than 0.003, which implies that the improved model should be safely protected against any cracks or flakes of concrete.

## References

- ACI 318-11. Building code requirements for structural concrete.* American Concrete Institute (ACI), USA, 2011.
- Cowan, H. J.; Smith, P. R. 2004. *Dictionary of architectural and building technology.* 4<sup>th</sup> ed. New York: Spon Press, 34, 107.
- Harris, H. G.; Sabnis, G. M. 1999. *Structural modeling and experimental techniques.* 2<sup>nd</sup> ed. Boca Raton: CRC Press, 41–83. <http://dx.doi.org/10.1201/9781420049589>
- Harris, H. G.; Srikanth, L. 1980. Full-scale tests on horizontal joints of large panel precast concrete buildings, *PCI Journal* (March–April): 72–92. <http://dx.doi.org/10.15554/pcij.03011980.72.92>
- Hal, A.; Steve, H.; Paul, G.; Ronald, J. R. 1991. Design of stiff, low-vibration floor structures, *International Society for Optical Engineering (SPIE)* 1619: 180–191.
- Hong, K. P.; Lee, S. S.; Kwon, Y. H.; Chun, H. M.; Cho, K. S.; Kim, S. J. 2010. PC floor systems for microelectronics manufacturing buildings, in *Proc. of 4<sup>th</sup> International Conference on Experimental Mechanics*, 18–20 November 2009, Singapore, Vol. 7522, 75225M 1–9.
- Kim, S. J.; Lee, S. S.; Chun, H. M.; Hong, K. P. 2009. A study on the sub-micro vibration reduction floor system of the long-span structure for technology facilities, *Journal of Architectural Institute of Korea (Structural Division)* 25(10): 67–74.
- Korea Concrete Institute (KCI). 2007. *Structural concrete design code.* Korea.
- Korean Society of Architectural Hybrid System (AHS). 2007. *Precast concrete.* 1<sup>st</sup> ed. Seoul: Kimoonang, 25–30.
- Lee, S. S.; Chun, H. M.; Kim, J. G.; Hong, K. P. 2010a. Suggestions of segmented PC frame systems for the long span floor of anti-vibration industrial buildings, *Journal of Architectural Institute of Korea (Structural Division)* 26(11): 13–20.
- Lee, S. S.; Chun, H. M.; Kim, S. J.; Hong, K. P. 2010b. An experimental study on the assembly-workability of both-end cantilevered PC-beam to PC-column, and its structural behavior under eccentric load, *Journal of Architectural Institute of Korea (Structural Division)* 26(12): 57–64.
- Murray, T. 1975. Design to prevent floor vibrations, *AISC Engineering Journal* 12(3): 82–87.
- Nilson, A. H.; Darwin, D.; Dolan, C. W. 2003. *Design of concrete structures.* 13<sup>th</sup> ed. New York: McGraw-Hill, 617–633.
- Park, Y. G.; Song, H. B.; Lee, W. H.; Ryu, J. C.; Cho, S. G.; Lee, J. H. 2005. Development of a Segmented PC Beam System, *60<sup>th</sup> Architectural Institute of Korea Conference* 25(1): 313–316.

**Sijun KIM.** A PhD Student in the Department of Architectural Engineering, Yonsei University, South Korea. He received his MS degree in Architectural Engineering from Yonsei University. His main research interests are the performance evaluation of vibration control and long span PC structure system.

**Seongsoo LEE.** A Professor in the Department of Architecture and Building Engineering, Kunsan National University, South Korea. He received his PhD degree in Architectural Engineering from Yonsei University. His main research interests are long span PC system and vibration control.

**Homin CHUN.** A Professor in the Department of Architecture, Chodang University, South Korea. He received his PhD degree in Architectural Engineering from Yonsei University. His main research interests are vibration control and estimation of dynamic load.

**Kappyo HONG.** A Professor in the Department of Architectural Engineering, Yonsei University, South Korea. He received his PhD degree in Civil Engineering from The Ohio State University. His main research interests are earthquake resistant design, vibration control, composite beam, and PC structure system.